

Dielectric constant model for environmental effects on the exciton energies of single wall carbon nanotubes

A. R. T. Nugraha,^{1,a)} R. Saito,¹ K. Sato,¹ P. T. Araujo,² A. Jorio,² and M. S. Dresselhaus³

¹Department of Physics, Tohoku University, Sendai 980-8578, Japan

²Departamento de Física, Universidade Federal de Minas Gerais, Belo Horizonte 30123-970, Brazil

³Department of Physics, Massachusetts Institute of Technology, Cambridge, Massachusetts 02139-4307, USA

(Received 20 April 2010; accepted 29 July 2010; published online 1 September 2010)

The excitonic optical transition energies E_{ii} of single wall carbon nanotubes, that are modified by surrounding materials around the tubes (known as the environmental effect), can be reproduced by defining a dielectric constant κ which depends on the subband index, nanotube diameter, and exciton size. The environmental effects on excitons can be recognized on a plot of the functional form of κ simply by the different linear slopes obtained for different samples. This treatment should be very useful for calculating E_{ii} for any type of nanotube environment, hence providing an accurate assignment of many nanotube (n, m) chiralities. © 2010 American Institute of Physics.

[doi:10.1063/1.3485293]

Excitonic effects in carbon nanotubes have explained the optical transition energies of single wall carbon nanotubes (SWNTs) even at room temperature, since the exciton binding energies in one-dimensional (1D) materials become large, up to 1 eV.^{1–5} Measurements of such optical transition energies in photoluminescence or in the Raman excitation profile of the radial breathing modes (RBM) are useful for assigning the chiralities of SWNTs, which are denoted by a pair of integers (n, m).⁶ The excitonic transition energies E_{ii} for a SWNT, where $i=1, 2, 3, \dots$ specify the optical transitions between the i -th valence subband and the i -th conduction subband, are found to be strongly affected by a change in the surrounding materials around the SWNT, through the so-called environmental effect.⁷ While the RBM frequency has been understood by some empirical formulas,^{8,9} the remaining issues regarding the environmental effect are how significant are the different environments that modify the E_{ii} values for a given SWNT, and how such values can be reproduced accurately by a particular theoretical formulation. In some well-established methods used to synthesize carbon nanotubes, such as the “super-growth” (SG),¹⁰ “alcohol-assisted” (AA) chemical vapor deposition,¹¹ and the high pressure gas-phase decomposition of CO (HiPco) methods,¹² the experimental E_{ii} values observed for AA and HiPco tubes are redshifted when compared to those for SG tubes.¹³ The “Kataura” plot,^{14,15} which gives E_{ii} as a function of nanotube diameter d_t , is different for one particular environment relative to another, and therefore the environmental effect must be taken into account explicitly.

The environmental effect for E_{ii} can be explained in terms of the excitonic dielectric screening effect. Previous theoretical studies of E_{ii} mostly described the screening effect by a static dielectric constant κ which consists of screening terms by the surrounding materials (κ_{env}) and by the nanotube itself (κ_{tube}). Calculations by Jiang *et al.*¹⁶ using a constant $\kappa=2.22$ provided a good description for the optical transition energies of bundled SWNTs for a limited range of d_t .¹⁷ In parallel, Miyauchi *et al.*¹⁸ used $1/\kappa=C_{\text{tube}}/\kappa_{\text{tube}}+C_{\text{env}}/\kappa_{\text{env}}$, where C_{tube} and C_{env} are d_t -dependent coeffi-

cients, and thereby reproduced some experimental E_{ii} values, though only for a very limited number of E_{11} transitions for semiconducting SWNTs. Other sophisticated theoretical models on this subject have also been presented^{19,20} but these formulations might be too complicated for practical use. Recently, Araujo *et al.*²¹ reported a d_t -dependent κ that could reproduce many experimental E_{ii} values and thus represents a breakthrough toward tackling environmental effects. However, different κ dependencies on d_t were obtained for ($E_{11}^S, E_{22}^S, E_{11}^M$) relative to (E_{33}^S, E_{44}^S), where S (M) denotes semiconducting (metallic) SWNTs. In the present work, we show a significant improvement in the theoretical treatment of the κ function. This treatment can unify all the dependencies for ($E_{11}^S, E_{22}^S, E_{11}^M, E_{33}^S, E_{44}^S$) over a broad range of d_t ($0.7 < d_t < 2.5$ nm). Now κ is found not only to depend on d_t but also on the exciton size l_k in reciprocal space. We then establish an empirical formula to calculate unknown E_{ii} for different sample environments. Here, we adopt the experimental E_{ii} values of resonant Raman excitation profiles for SG,^{13,21} AA,²¹ and HiPco based SWNTs.⁷ We focus the environmental effect only on the surfactant materials of SWNTs which are important for the isolation and dispersion of SWNTs. Other effects, such as local impurity and exciton-phonon interactions may modify the exciton properties. However, such effects may not be scaled as a function of diameter or exciton size.

The details of the exciton energy calculation used here have been described in the previous papers.^{16,17} E_{ii} is calculated as a transition from the ground state to the first bright exciton state by solving the Bethe–Salpeter equation within the extended tight-binding (ETB) model. The ETB model includes curvature and many-body effects. Including the Coulomb interaction in the many-body terms is essential for considering the environmental effect, since the shift of E_{ii} is understood by the change of κ in the screened Coulomb potential, which is expressed as $W=V/\kappa\epsilon(\vec{q})$, where V is the unscreened Coulomb potential modeled by the Ohno potential^{1,22} and $\epsilon(\vec{q})$ is the dielectric function for the π electrons. The effect of electrons in core states, σ bonds, and the surrounding materials are all represented by a single parameter κ .¹⁶ In Fig. 1, E_{22} versus κ is plotted for a (9,7) SWNT.

^{a)}Electronic mail: nugraha@flex.phys.tohoku.ac.jp.

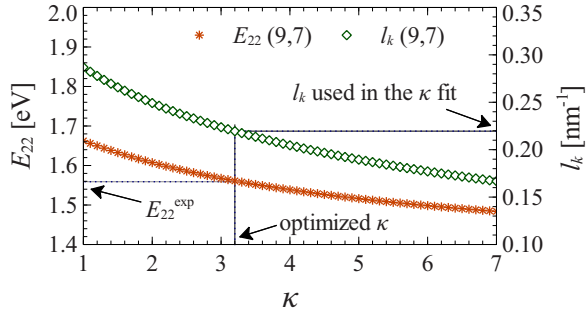


FIG. 1. (Color online) Left and right vertical axes show, respectively, the E_{22} and l_k dependences on κ for a (9,7) SWNT. The plot shows how the optimized κ is obtained for a given SWNT in a HiPco sample (data from Ref. 7).

From the plot, one can get an “optimized” κ that reproduces the experimental E_{22} value (E_{22}^{exp}). The plot also gives the related l_k (l_k^{-1}) denoting the respective exciton size in reciprocal (real) space. The exciton size is given by the full width at half maximum of the exciton wave function profile in 1D k -space.¹⁶ Repeating this procedure for many (n,m) and E_{ii} values for several samples, we obtain a set of optimized κ values for the different samples. Using these optimized κ values, a general κ function is modeled to have the functional form

$$\kappa \approx C_\kappa [p^a (1/d_t)^b (1/l_k)^c], \quad (1)$$

where the integer p corresponds to the ratio of the distances of the cutting lines for each E_{ii} transition from the K point in the two-dimensional Brillouin zone of graphene,¹⁵ and $p = 1, 2, 3, 4, 5$ stands for E_{11}^S , E_{22}^S , E_{11}^M , E_{33}^S , and E_{44}^S , respectively. The variable l_k is involved in the κ function because of the screening by the different environments which modify l_k . The parameters (a, b, c) thus determined are common for all different samples so as to both optimize the correlation between κ and (p, d_t, l_k) , and to minimize differences between theory and experiment.

In Fig. 2, we show a series of results for the κ function for different samples. For each sample, we can unify the κ

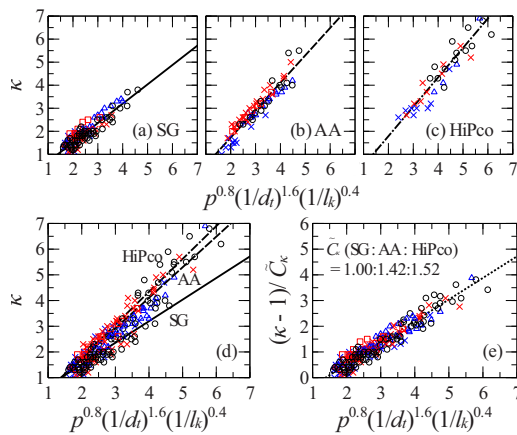


FIG. 2. (Color online) The κ function for (a) SG, (b) AA, and (c) HiPco samples. (d) Data for all three samples are plotted with a fitted slope C_κ for each sample. (e) All the κ functions collapse on to a single line after dividing each function with the corresponding \tilde{C}_κ . The following symbols are used: E_{11} (\circ), E_{22} (\times), E_{33} (\triangle), E_{44} (\square). Black, red, and blue colors, respectively, denote metallic [$\text{mod}(2n+m, 3)=0$], semiconducting type I [$\text{mod}(2n+m, 3)=1$], and type II [$\text{mod}(2n+m, 3)=2$] SWNTs. See Ref. 24 for supplementary material.

function for the lower transitions ($E_{11}^S, E_{22}^S, E_{11}^M$) and higher transitions (E_{33}^S, E_{44}^S), and we note that this unity was missing in previous work.²¹ Considering l_k explicitly in our work is important to properly describe the environmental effect. Indeed, the exciton size is a key variable in the dielectric screening of excitons. Keeping d_t constant, the κ values for higher E_{ii} are smaller than those for lower E_{ii} . Thus l_k^{-1} (the exciton size in real space) is also smaller because only a small amount of the electric field created by an electron-hole pair will influence the surrounding materials. If l_k for a particular E_{ii} is kept constant, tubes with a smaller d_t will experience a stronger dielectric screening effect because the electric field lines from the electron-hole pair can easily go outside of the tube, thus explaining why both d_t and l_k need to be taken into account in the κ formulation. The values of (a, b, c) from the best fitting result are found to be $(0.80 \pm 0.10, 1.60 \pm 0.10, 0.40 \pm 0.05)$, respectively. This somehow indicates another scaling relation of excitons similar to the previously reported scaling law, which relates the binding energy E_{bd} with d_t , κ , and the “effective mass” μ .²² If we adopt $E_{\text{bd}} \propto \mu^{\alpha-1} d_t^{\alpha-2} \kappa^{-\alpha}$ with $\alpha=1.40$ as is given by Eq. (7) in Ref. 22, we can obtain the form of Eq. (1) by making a conversion of variables from $E_{\text{bd}}(\mu, d_t, \kappa)$ to $\kappa(p, d_t, l_k)$. It is also found that if we replace l_k in Eq. (1) by μ , two scaling relations will be needed, one for M-SWNTs and another for S-SWNTs. This is because E_{bd} for an M-SWNT is screened by free electrons even for a similar μ value for the photoexcited carriers. Using l_k in the κ function thus gives us a unified scaling relation for both M- and S-SWNTs. The scaling law itself originates from the nature of the Coulomb potential that always scales with some size parameters.

Looking carefully at the plots for each sample in Fig. 2, the only difference we can find between the various plots is the slope or gradient C_κ of the κ function. Values C_κ for the SG, AA, and HiPco samples are 0.84, 1.19, and 1.28, respectively, where we omit the units of C_κ . We expect that such differences arise from the environmental effects on the exciton energies. Therefore, we assume each C_κ characterizes the environmental dielectric constant κ_{env} of each sample. The argument is as follows. As discussed in Ref. 20, κ can be modeled in analogy to a series connection of two capacitors, one for the tube (κ_{tube}) and another one for the environment (κ_{env}). For a given SWNT, the tube term κ_{tube} remains the same and the environment term κ_{env} is modified when κ changes. The difference in C_κ must then come from the difference in κ_{env} . The SG sample has the largest E_{ii} and hence the smallest κ relative to any other samples discussed in the literature,¹³ so for simplicity we normalize C_κ of the SG sample to be $\tilde{C}_\kappa(\text{SG})=1.00$. The values of \tilde{C}_κ for the other samples can then be determined by taking the ratio of their C_κ to that for the SG sample. Thus \tilde{C}_κ for the SG, AA, and HiPco samples becomes 1.00, 1.42, and 1.52, respectively. If we now plot the ratio κ/\tilde{C}_κ for each sample, it is found that all points collapse on to a single line, as shown in Fig. 2(e). This fact gives further support for the use of \tilde{C}_κ as a unique parameter for each environment. This treatment has been checked to work for many surrounding materials, and the justification of the treatment will be reported elsewhere.

With the knowledge of \tilde{C}_κ for several types of environments, we can use these results in practical applications. To a

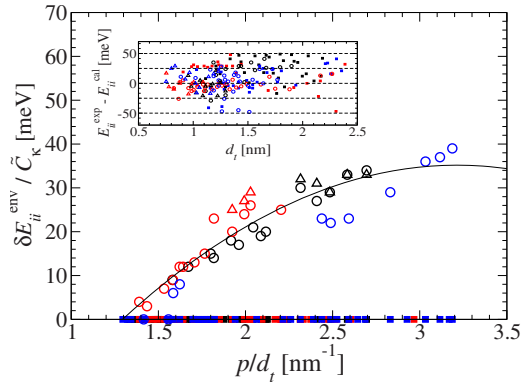


FIG. 3. (Color online) $\delta E_{ii}^{\text{env}} / \tilde{C}_\kappa$ vs d_t , scaled by \tilde{C}_κ . Circles and triangles, respectively, denote AA and HiPco samples. Many square symbols on the zero line denote the SG sample which is taken as the standard. The inset shows differences between experimental (exp) and calculated (cal) E_{ii} values for many samples, showing good agreement between experiment and our model.

first approximation, we fit the energy shift $\delta E_{ii}^{\text{env}}$ due to different environments (Fig. 3) by

$$\delta E_{ii}^{\text{env}} = E_{ii}^{\text{SG}} - E_{ii}^{\text{env}} \equiv \tilde{C}_\kappa \left[A + B \left(\frac{p}{d_t} \right) + C \left(\frac{p}{d_t} \right)^2 \right], \quad (2)$$

where A , B , C , are parameters common to all types of environments and E_{ii}^{env} is calculated with the κ function obtained in Eq. (1).²³ We find the best fit for $A = -42.8$ meV, $B = 46.34$ meV nm, $C = -7.47$ meV nm². The SG sample is then fixed as a standard, and all E_{ii} values for the other environments can be calculated simply by $E_{ii}^{\text{env}} = E_{ii}^{\text{SG}} - \delta E_{ii}^{\text{env}}$, given by Eq. (2). This treatment thus provides a general way to obtain the Kataura plot for SWNTs in any type of environment within an accuracy of 50 meV for all energy regions and d_t values (see inset of Fig. 3 and Ref. 24).

In summary, we have developed the κ function for SWNTs surrounded by several different types of materials using a simple dielectric constant model. The results show a consistent picture for an exciton scaling law in carbon nanotubes. Moreover, the environmental dielectric constant obtained within our treatment can be used to reproduce many experimental E_{ii} values for SWNTs found in different environments.

A.R.T.N. is supported by a MEXT scholarship. R.S. and K.S. acknowledge MEXT Grant No. 20241023. We are very

grateful for fruitful discussions with Professors Y. Ohno and S. Maruyama. The Brazilian authors acknowledge MCT-CNPq and the AFOSR/SOARD Project (Award No. FA9550-08-1-0236). The MIT author acknowledges NSF Grant No. DMR-07-04197.

¹T. Ando, *J. Phys. Soc. Jpn.* **66**, 1066 (1997).

²C. D. Spataru, S. Ismail-Beigi, L. X. Benedict, and S. G. Louie, *Phys. Rev. Lett.* **92**, 077402 (2004).

³F. Wang, G. Dukovic, L. E. Brus, and T. F. Heinz, *Science* **308**, 838 (2005).

⁴J. Maultzsch, R. Pomraenke, S. Reich, E. Chang, D. Prezzi, A. Ruini, E. Molinari, M. S. Strano, C. Thomsen, and C. Lienau, *Phys. Rev. B* **72**, 241402 (2005).

⁵M. S. Dresselhaus, G. Dresselhaus, R. Saito, and A. Jorio, *Annu. Rev. Phys. Chem.* **58**, 719 (2007).

⁶R. Saito, G. Dresselhaus, and M. S. Dresselhaus, *Physical Properties of Carbon Nanotubes* (Imperial College Press, London, 1998).

⁷C. Fantini, A. Jorio, M. Souza, M. S. Strano, M. S. Dresselhaus, and M. A. Pimenta, *Phys. Rev. Lett.* **93**, 147406 (2004).

⁸P. T. Araujo, C. Fantini, M. M. Lucchese, M. S. Dresselhaus, and A. Jorio, *Appl. Phys. Lett.* **95**, 261902 (2009).

⁹P. T. Araujo, P. B. C. Pesce, M. S. Dresselhaus, K. Sato, R. Saito, and A. Jorio, *Physica E (Amsterdam)* **42**, 1251 (2010).

¹⁰K. Hata, D. N. Futaba, K. Mizuno, T. Namai, M. Yumura, and S. Iijima, *Science* **306**, 1362 (2004).

¹¹S. Maruyama, R. Kojima, Y. Miyauchi, S. Chiashi, and M. Kohno, *Chem. Phys. Lett.* **360**, 229 (2002).

¹²P. Nikolaev, M. J. Bronikowski, R. K. Bradley, F. Rohmund, D. T. Colbert, K. A. Smith, and R. E. Smalley, *Chem. Phys. Lett.* **313**, 91 (1999).

¹³P. T. Araujo and A. Jorio, *Phys. Status Solidi B* **245**, 2201 (2008).

¹⁴H. Kataura, Y. Kumazawa, Y. Maniwa, I. Umezui, S. Suzuki, Y. Ohtsuka, and Y. Achiba, *Synth. Met.* **103**, 2555 (1999).

¹⁵R. Saito, G. Dresselhaus, and M. S. Dresselhaus, *Phys. Rev. B* **61**, 2981 (2000).

¹⁶J. Jiang, R. Saito, G. G. Samsonidze, A. Jorio, S. G. Chou, G. Dresselhaus, and M. S. Dresselhaus, *Phys. Rev. B* **75**, 035407 (2007).

¹⁷K. Sato, R. Saito, J. Jiang, G. Dresselhaus, and M. S. Dresselhaus, *Phys. Rev. B* **76**, 195446 (2007).

¹⁸Y. Miyauchi, R. Saito, K. Sato, Y. Ohno, S. Iwasaki, T. Mizutani, J. Jiang, and S. Maruyama, *Chem. Phys. Lett.* **442**, 394 (2007).

¹⁹V. M. Adamyan, O. A. Smyrnov, and S. V. Tishchenko, *J. Phys. Conf. Ser.* **129**, 012012 (2008).

²⁰T. Ando, *J. Phys. Soc. Jpn.* **79**, 024706 (2010).

²¹P. T. Araujo, A. Jorio, M. S. Dresselhaus, K. Sato, and R. Saito, *Phys. Rev. Lett.* **103**, 146802 (2009).

²²V. Perebeinos, J. Tersoff, and P. Avouris, *Phys. Rev. Lett.* **92**, 257402 (2004).

²³In using the κ function of Eq. (1), the input l_k should be determined self-consistently to the calculated l_k . However, we adopt l_k from the optimized κ value as shown in Fig. 1 for simplicity. In fact, l_k is a slowly changing function of κ .

²⁴See supplementary material at <http://dx.doi.org/10.1063/1.3485293> for a list of E_{ii}^{SG} as the standard values.